FULL PAPER

A novel conducting polyamic acid/nanocomposite coating for corrosion protection

Rawaa Abbas Mohammed* |Khulood A. Saleh

Department of Chemistry, Science College, Baghdad University, Baghdad, Iraq

Corrosion are of paramount interests to a researcher due to their important impacts on both people's safety and economy. A recent strategy bases on a new material has been utilized for mitigating corrosions. Conducting polymer-based Nano composites are classes of material that can be promising for corrosion protection. PAA-Nano composites on mild steel (MS) and Electropolymerization of polyamic acid (PAA) was applied in monomer solutions by the techniques of constant potential. The protection property of coating was investigated in 3.5% solution of NaCl by Tafel polarizations at varied temperature (293 - 323K). The effect of varied Nano materials (ZnO and Graphen (G)) upon the protections performances of the Nano composite coating were compared. The results revealed that PAA/Nano composite and PAA provides the best performances for corrosions protections of the MS by reducing its corrosions current densities in comparison with the blank MS. In addition, this coating is featured by AFM, and FT-IR, SEM method. Also ‹the effect of increasing temperature presented as thermodynamic and kinetic parameters {Ea, ΔH*, ΔS*, and ΔG*}, were calculated and discussed.

*Corresponding Author:
Rawaa Abbas Mohammed
Email:rawaa.a.mohammed@sc.uobaghdad.edu.iq
Tel.: +0096 07902164596

Introduction

Corrosion of metal is the phenomenon that pertains to the destruction of metallic materials by the surroundings mediums. Recently, metals corrosion has turned into a common problem encountered by many countries around the globe, because they greatly reduce the mechanical property of metals material and the services lives of metals equipment. So, metal corrosions should be controlled and prevented. Among the many anti corrosion methods, anti-corrosives coating are kinds of simple, effective, very extensive, and economical methods [1,2]. Nowadays, conducting polymer coating and Nano polymer composites coating are used widely in various projects. Studies on Nano polymer composites coating, conducting polymer and their combination have been conducted with good progress. Regarding some novel nontoxic corrosion protection materials, besides the property of good efficiencies and smart corrosions protections, long periods of effectiveness and easy constructions have been improved. The coatings have different deposition mechanisms, such as physical vapors deposition {PVD}, chemical vapor deposition {CVD}, sol gel, thermal spray, micro arc oxidation (MAO), electro-deposition and electro-chemical deposition coating [3,4]. Wide ranges of electro chemical techniques

could be utilized for electro chemical polymerizations, but galvanostatic (constants currents), potentiostatic (constants potentials) and potential sweeping technique, like cyclic voltammetry, is the method that is frequently conducted [5]. Here, the focus is on conducting polymers coating and Nano polymer composites coating. Coatings with the property of long terms corrosions resistances, strong adhesions, better durability and good surfaces mechanical abrasions were in good demands. It was proven that utilizing Nano particles in utilizing polymers coating can not only fill the pore for enhancing the barriers effects but also enhances the electro chemical anticorrosion and other performance like adhesions, thermal stabilities, mechanical strengths, magnetonstatic shielding and hydrophobic properties [6-10]. Many types of Nano particles like Zn, TiO_2, Si, ZnO, Al_2O_3, CeO_2, SiO_2, Nano clays and Nano tubs were added in polymers coating and revealed better protective behaviors than ordinary polymer coating. Graphene is hexagonal honeycombs two-dimensional crystal material made of sp^2 carbons [11-13], widely utilized in many fields recently because of its good electrical and thermal conductivities, sheets structures, Nontoxic and barriers properties; this property provides good theoretical bases for the research on graphene in anti-corrosive coating [14,15].

In this study, polyamic acids/Nano material (ZnO NPs and Graphen (G)) Nano composites were synthesized electrochemically on Mild Steels (MS). Then the protective performances of this coating against corrosions were measured by electrochemical polarizations techniques in 3.5% NaCl solutions at temperatures ranges of 293-323K.

Experimental part

Pre-treatment of Mild Carbon Steel {MS}

Mild Steel {MS}, containing 0.0855 wt % (C), <0.0100 wt % (Si), 0.199 wt % (Mn), 0.0341

wt % (Cr), <0.0050 wt % (Mo), 0.0250 wt % (Ni) and iron (Fe), has the remaining percentage, which is about 99.5 wt %. The operating electrode was made of a circular piece {2.5 cm * 2 mm}. Before the experiment, it was mechanically polished with varied SiC paper {600, 800, 1000, 1200 and 2000 grit}, then cleaned with acetone, distill water and degreased, finally dried at room temperature.

Chemical

Sulfuric acid {H_2SO_4, CDH, 98%}, sodium chloride {NaCl, BDH, 99%}, acetone {C_3H_6O, Alpha (α), 99%}, Znic Oxide Nano particles {ZnO NPs} and Graphene {G} were purchased from US research Nano materials Inc. (USA) and Sky spring Nano materials Inc. (USA), respectively. Any solution in the study was made by distilled water.

Electropolymerization on MS

The electro polymerization of N-[(1H-Indol-3-yl)-2-ethyl] maleamic acid as monomer onto the {MS} surface was conducted in the monomer solution utilizing {DC} power supply and two electrodes, namely the working electrodes {WE} and the countries electrodes {CE} (Galvano static techniques). The solution implemented for electro chemical polymerization consisted of 0.1 g of monomer in 100 ml H_2O with five drops of H_2SO_4 [16]. For corrosion measurements, MS was utilized as a {WE}, platinum as auxiliary electrodes, and saturated calomel electrodes (SCE) as references electrodes. Anodic and Cathodic and polarizations of MS were conducted under potentiostatic condition in 3.5% NaCl solution and at temperatures ranges of 293-323 K. Furthermore, 0.04 g of ZnO NPs and 0.01 g of graphene were placed for increasing the efficiencies of polymer films to prevent corrosion. Equation 1 shows the electro chemical polymerization for the monomer.

N-[(1H-Indol-3-yl)-2-ethyl] maleamic acid → Polymerization → Poly (N-[(1H-Indol-3-yl)-2-ethyl] maleamic acid)
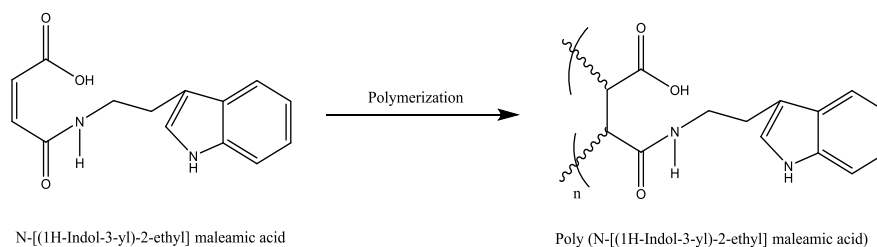
EQUATION 1 Conversion of the monomer to polymer

Characterization

The polymer and polymer nanocomposites deposited layers were subjected to morphologic and spectroscopic tests by scanning electron microscope (SEM) of Shimadzu model S-4160, FTIR of Shimadzu model 3600.

Results and discussions

Polymerization mechanism

The cationic mechanism [17,18] explain the electro chemical polymerization processes, as shown below.

Cationic mechanism (Scheme1): The applications of the anodic potentials to the monomer solution found in below:

[A1]: transferring an electron from the monomer to the electrode;

[A2]: transferring an electron in A1 leads to the formation of radical cation that is adsorbed on the surface of the electrode;

[A3]: the radical cation was reacted and adsorbed in the solution for increasing weight of the molecular of the species; and

[A4]: the monomer molecule is put by the mechanism of the cationic of the oxidized monomer charged ends.
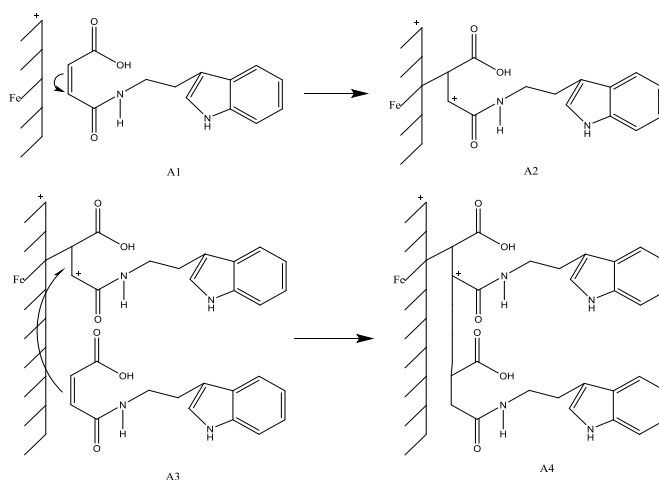

SCHEME 1 Cationic mechanism of polymer film on MS

Fourier transmission infrared (ft-ir) spectroscopy

In accordance with Figure 1A for monomer, the band shown at {1639.38} cm^{-1} was for C=O of the amide groups, the band shown at {1712.26} cm^{-1} was for C=O of carboxylic acid, the band of NH of amide was shown at {3197.76} cm^{-1}, the band of OH of carboxylic acid was shown at {2596.01} cm^{-1}, the band of aromatic C=C was shown at {1502.44} cm^{-1}, and the band of secondary amine NH was shown at {3293.26} cm^{-1} [19-21].

The films of polymer were featured by FT-IR as revealed in Figure 1B. In this spectrum, the aliphatic double bond (=CH) 3100 cm^{-1} have vanished, proving the formation of polymer.
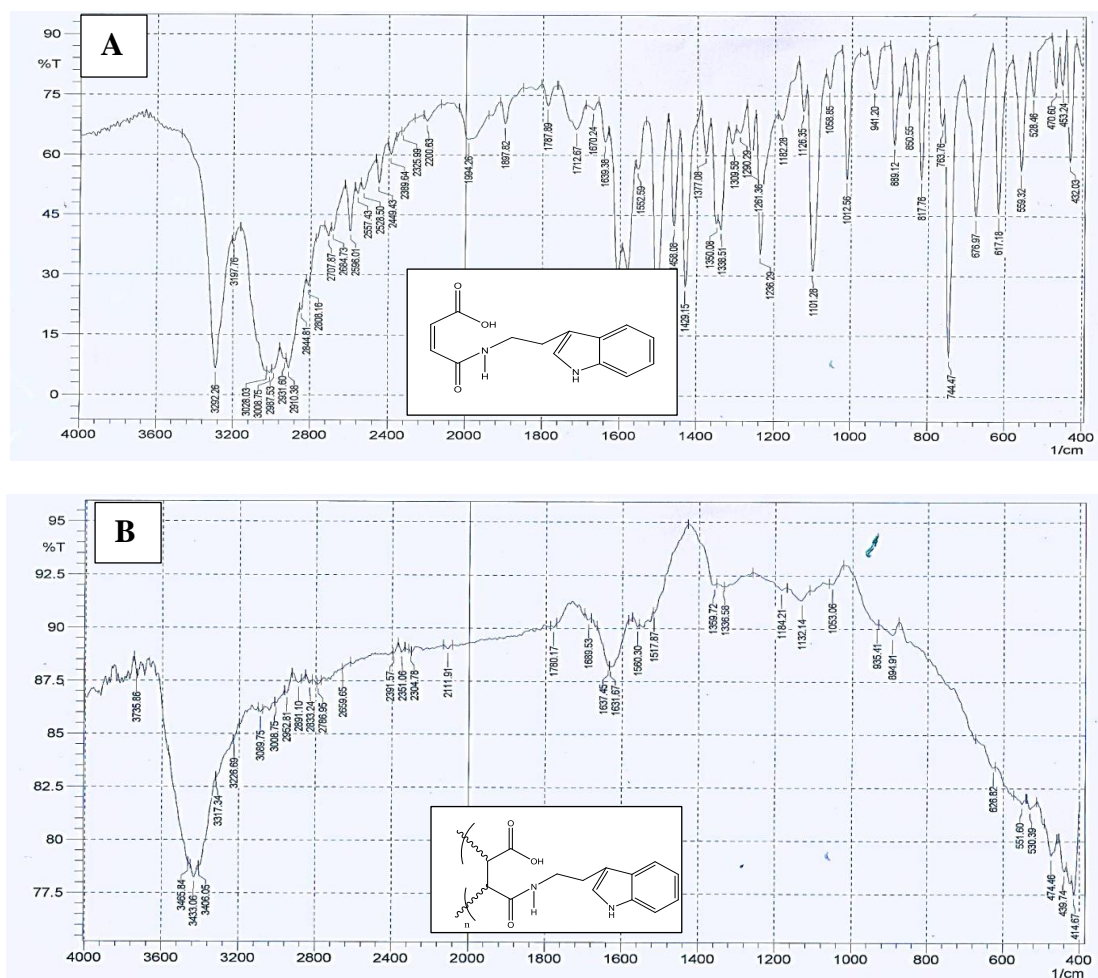
FIGURE 1 FT-IR for (A) monomer, (B) polymer

*Atomic force microscope (AFM)*

AFM is utilized for revealing further information, because of its functions as one of the surface investigations instruments for Nano scale structures. Figures 2A, 2B, and 2C show the 2 and 3 dimensions for the all set polymer in the presence and absences of the Nano materials. This image shows the degrees of agglomerations of the Nano materials, because of the ZnO NPs adhesive and G and to the polymer, besides the generated smoother layer. In AFM analyses, roughness average {Ra} and Root Mean Square Roughness {R.M.S} were the most widely utilized parameter for characterizing the surface roughness of the generated polymer film. The achieved R.M.S and Ra value is shown in Table 1. The results indicated a decrease in the surfaces roughness and an increase in the smoothness after modifications of the polymer with the Nano materials, because the reduction in the size of the grain leads to a rise in the effects of the energy barriers for protection against corrosion [22,23].

TABLE 1 The root mean square roughness {R.M.S} roughness average {Ra}, and medium grain sizes for coated MS by film of polymer in presence and the absences of the Nano materials

| System	Ra (nm)	R.M.S (nm)	Mean grain size (nm)
Coated MS with polymer	34.0	41.1	98.4
Coated MS with polymer + G	20.6	23.8	96.8
Coated MS with polymer + ZnO NPs	12.6	14.5	65.4
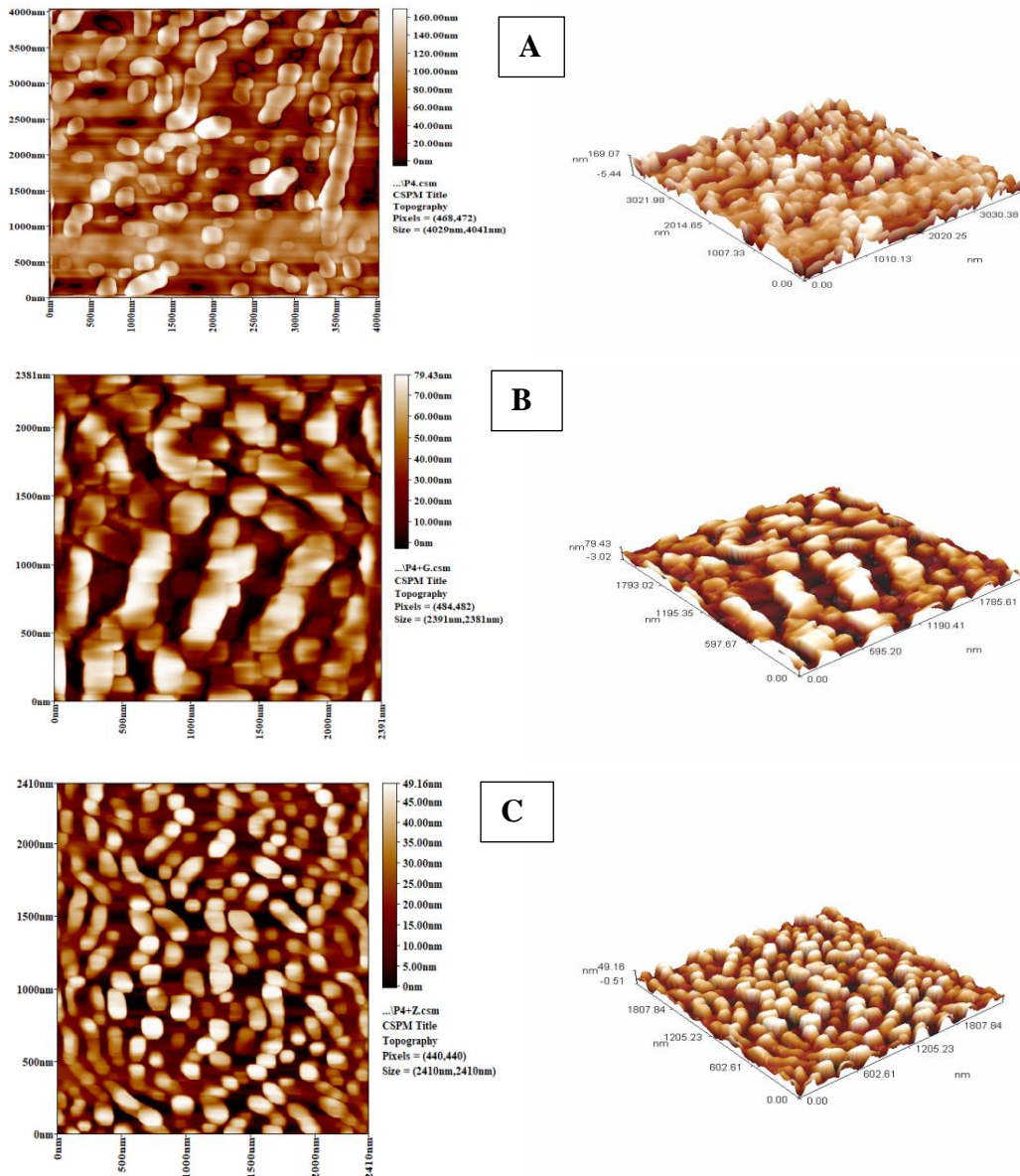
FIGURE 2 AFM images for (A) polymer, (B) polymer modified with G, (C) polymer modified with ZnO NPs

Scanning electrons microscopes (SEM)

The surface morphological property of polymer films in the presence and absence of the Nano materials are featured by scanning electron microscope {SEM}. Figure 3A reveals that the polymer coating has the spherical structure and the distribution of polymer balls is inhomogeneous on the surfaces of MS. Figure 3B reveals the polymer films modified with graphene, with the good interaction between the polymer matrixes and graphene besides the homogeneous distribution of the graphene sheet in the matrixes of the polymer [24]. Figure 3C reveals the polymer films amended with ZnO NPs, where ZnO NPs was uniformly scattered in the matrixes. ZnO NPs aggregation was seen at other location because of their hydrophilic nature and high specific surface area [25].
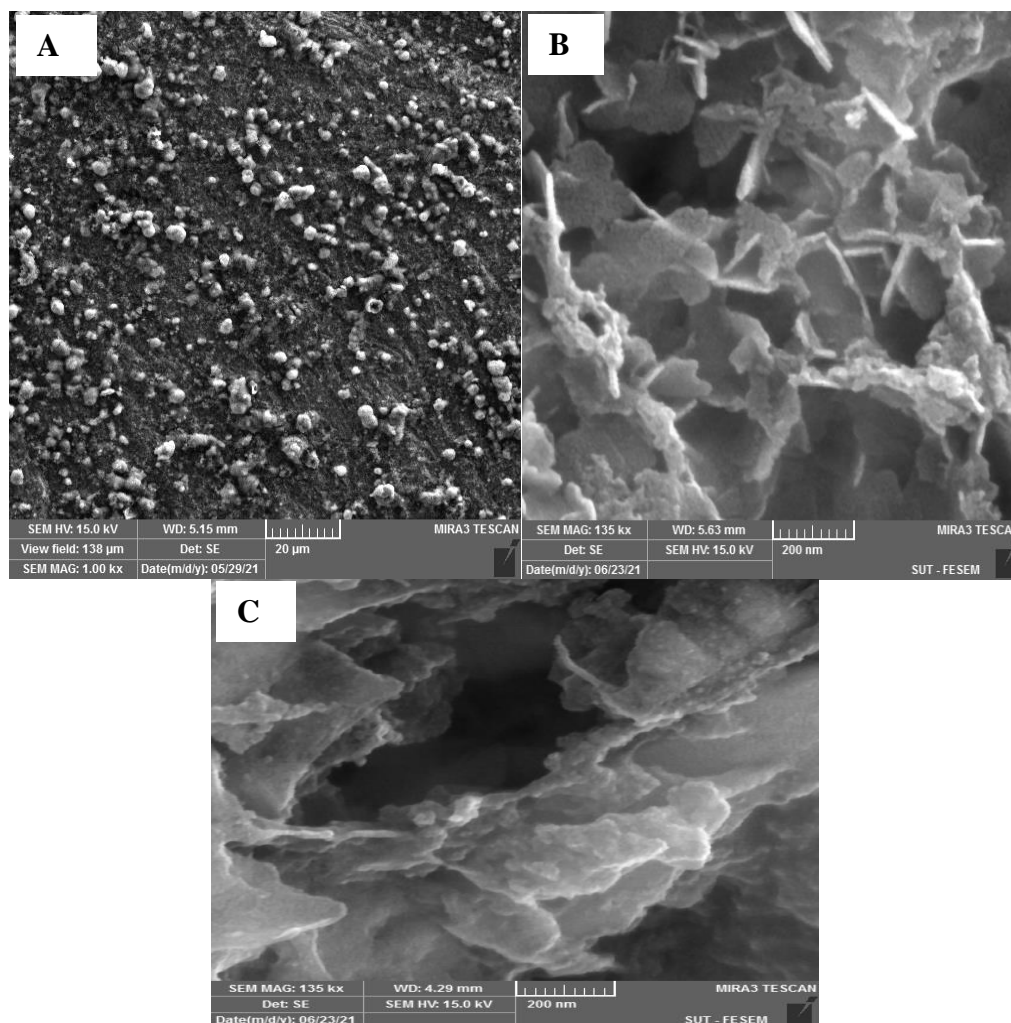
FIGURE 3 SEM images for A) coated MS by polymer film, B) coated MS by polymer film improved with G, C) coated MS with polymer film improved with ZnO NPs

Potentiostate polarization curves

Corrosion parameters are calculated by data resulted in Table 2 and Figure 4. The corrosion current density (icorr) and corrosion potential (Ecorr) are gained by the extrapolation of anodic and cathodic Tafel curves of coated and un-coated MS with polymer films in 3.5% NaCl solution. Cathodic (βc) and the anodic (βa) Tafel slope was also measured from Figure 4. Table 2 shows the resulted data of the corrosion potential Ecorr (mV), corrosion current density icorr (μA/cm²), anodic and cathodic Tafel slope βa and βc (mV/Dec), polarization resistance Rp (Ω/cm²), corrosion rate CR (g/m².d), corrosion penetration CP (mm/y), and protection efficiency PE%. The data in Table 2 shows that the corrosion current density (icorr) and corrosion potential (Ecorr) are generally raised with temperatures. Tafel plots reveal that Ecorr of the coated MS shift to higher positions in comparison with un-coated MS, which is an implication that the protection acts as the anodic protection [26]. The protection efficiency (%PE) is measured by Equation 1 below [27]:

$$\% \, PE = \frac{(icorr)o - (icorr)}{(icorr)o} * 100 \qquad (1)$$

In which $(icorr)_o$ stands for the corrosion current density for the uncoated MS, and (icorr) stands for the corrosion current density for the coated MS. The polarization resistance (Rp) is determined by Stern Gery Equation 2 [28]:

$$Rp = \frac{\beta a \beta c}{2.303\,(\beta a + \beta c)icorr} \qquad (2)$$

The polarization resistance (Rp) measurement has similar requirement to the measurement of the full polarization curves, which are useful methods for identifying corrosion upset and for initiating the remedial actions. The values of Rp are shown in Table 2.
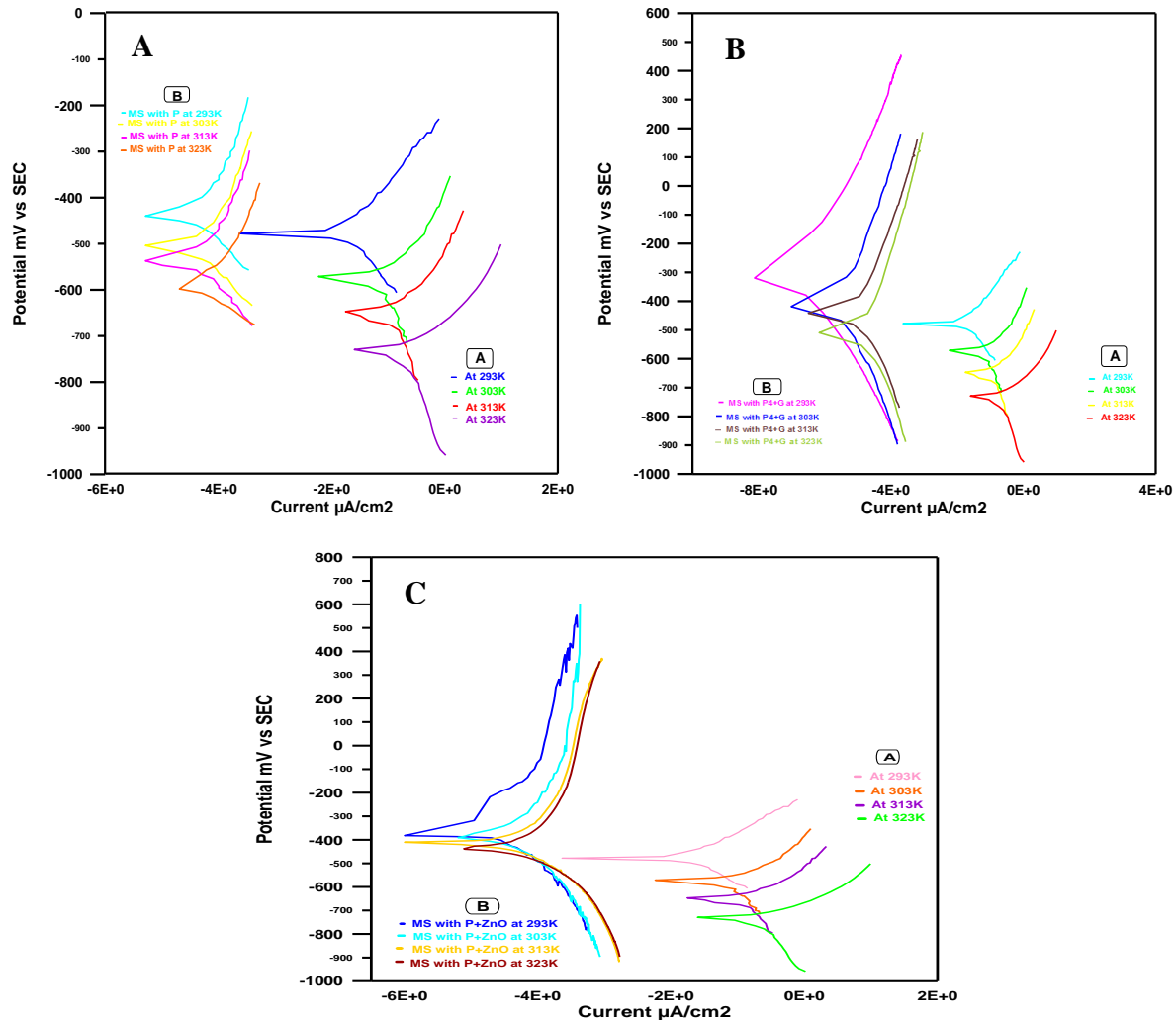
FIGURE 4 Polarization curves for corrosion of (A) uncoated MS & coated MS with polymer film, (B) uncoated MS & coated MS with polymer film+ Graphen (G), (C) uncoated MS & coated MS with polymer film + ZnO NPs

TABLE 2 Corrosion parameters for coated MS and uncoated MS with polymer film in presence and the absence of the Nano materials (G & ZnO NPs) in 3.5% NaCl solution

	T(K)	E_{corr} (mV)	i_{corr} (µA/cm²)	βc (mV/Dec)	βa (mV/Dec)	CR (g/m².d)	CP (mm/y)	PE%	R_p (Ω/cm²)
Uncoated MS	293	-471.8	24.1	-136.4	130.7	4.02	0.187	-	1202.6
	303	-572.1	79.7	-162.6	132.7	14.3	0.664	-	398.1
	313	-646.5	111.3	-186.7	148.5	28.7	1.33	-	322.7
	323	-676.8	133.2	-193.9	131.6	32.2	1.54	-	255.6
Coated MS with polymer	293	-443.5	0.417	-103.1	161.4	0.0069	0.00032	98.3	65509.8
	303	-503.9	0.685	-109.6	135.7	0.0072	0.00034	99.1	38433.4
	313	-536.3	0.801	-107.5	129.0	0.0086	0.00040	99.3	31786.3
	323	-592.5	0.936	-117.5	148.7	0.0107	0.00049	99.3	30448.9

Coated MS with polymer	293	-331.0	0.199	-516.7	613.7	0.0020	0.000093	99.2	612090.2
	303	-405.8	0.369	-525.5	523.5	0.0036	0.000168	99.5	308598.4
	313	-436.3	0.464	-536.1	525.8	0.0046	0.000216	99.6	248411.0
	323	-510.4	0.617	-523.4	628.2	0.0053	0.000307	99.5	200932.8
Coated MS with polymer +	293	-376.7	0.114	-372.4	470.4	0.0029	0.00013	99.5	791687.3
	303	-396.4	0.279	-385.3	499.5	0.0047	0.00044	99.7	338525.4
	313	-407.5	0.459	-443.1	503.4	0.0115	0.00053	99.6	222939.9
	323	-435.8	0.685	-594.9	772.0	0.0171	0.00079	99.5	212980.6

Thermo dynamic activation parameters and kinetic

Thermo dynamic activation parameters involve the activation energies Ea, activation enthalpy ΔH^*, and activation entropy ΔS^*, as measured by utilizing the Arrhenius equation and its alternatives formulations that are named as the transition states. The activation energy is determined from the plots that represent the relationship between the reciprocal of the absolute temperature and Log CR (1/T) [29], as revealed in Figure 5.

$$Log\ CR = Log\ A - \frac{Ea}{2.303\ RT} \qquad (3)$$

In which CR denotes corrosion rate, A is pre exponential factor, Ea signifies Activation energy, R refers to Gas constant (8.315 JK^{-1}mol^{-1}), and T shows absolute temperature (K). The transition states are shown in the Equation below [30]:

$$Log\ \frac{CR}{T} = Log\left(\frac{R}{Nh}\right) + \frac{\Delta S^*}{2.303R} - \frac{\Delta H^*}{2.303RT} \qquad (4)$$

Where N refers to Avogadro's number (6.022 × 10^{23} mol), and h stands for Plank constant (6.62 × 10^{-34} J.S). The activation entropy ΔS^* and activation enthalpy ΔH^* are decided from the plots which represent the relationship between the reci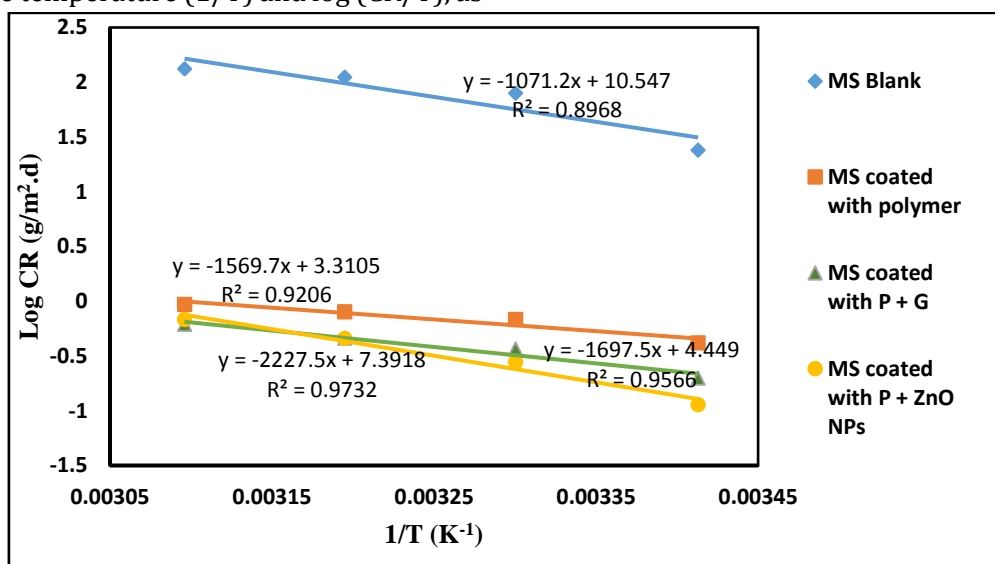procal of the absolute temperature (1/T) and log (CR/T), as 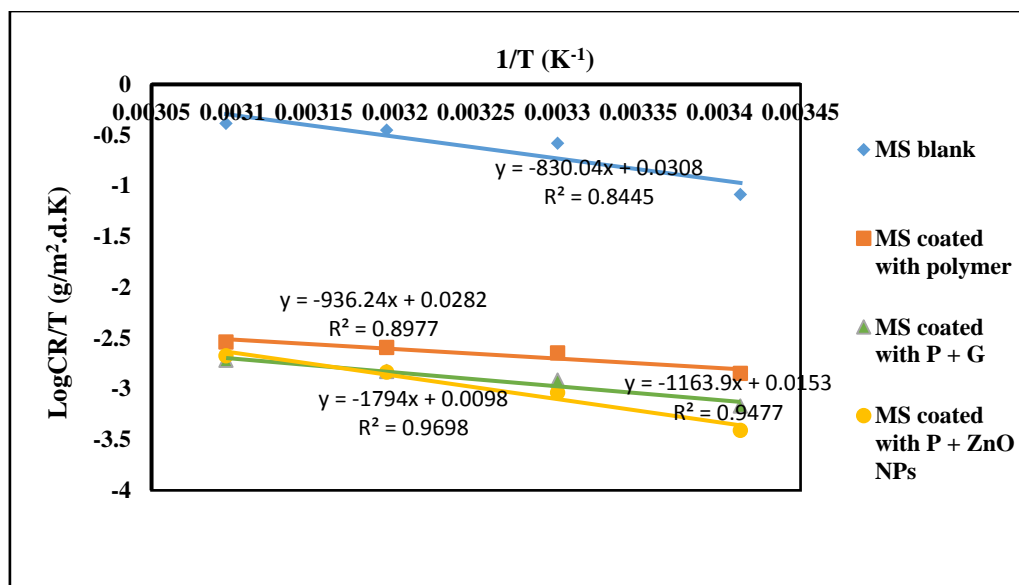revealed in Figure 6, in which the slope represents ($-\Delta H^*/2.303RT$) and the intercept represents (Log(R/Nh) + $\Delta S^*/2.303R$). The activation of free energy was decided from Equation 5 below:

$$\Delta G^* = \Delta H^* - T\Delta S^* \qquad (5)$$

FIGURES 5 Plots of log CR vs. 1/T for the coated and uncoated MS with polymer film in the presence and absence of the Nano materials (G and ZnO NPs) in 3.5% NaCl solution

FIGURE 6 Plots of log CR/T vs. 1/T for the coated and uncoated MS with polymer film in the presence and absence of the Nano materials (G and ZnO NPs) in 3.5% NaCl solution

TABLE 3 Thermo dynamic parameters at varied temperatures for the corrosion of the coated and uncoated MS with polymer film in the presence and absence of the Nano materials (G & ZnO NPs) in 3.5% NaCl solution

T(K)		Ea (kJ/mole)	ΔH* (kJ/mol)	ΔS* (J/mol.K)	ΔG* (kJ/mol)
Uncoated MS	293	20.5	15.9	-196.9	73.6
	303				75.6
	313				77.5
	323				79.5
Coated MS with polymer	293	30.1	17.9	-197.0	75.6
	303				77.6
	313				79.6
	323				81.5
Coated MS with polymer + G	293	32.5	22.3	-197.3	80.1
	303				82.1
	313				84.1
	323				86.0
Coated MS with polymer + ZnO NPs	293	42.7	34.3	-197.4	92.1
	303				94.1
	313				96.1
	323				98.1

Generally, the data show that the thermo dynamic activation parameters (Ea and ΔH*) for the MS coated by the polymer film were bigger than those of the uncoated MS. These indicate the rise in the energy barrier [31]. The value of the entropy of activation for the polymer film uncoated and coated MS was negative, suggesting that the activated complexes in the rate determined step were

gained in association instead of dissociation step, beside raised disordering which occur when moving from reactant to activated complexes [32]. The free energies activation has positive value, as revealed in Table 3. Furthermore, almost small changes were observed with increasing temperatures, which is an indication that the activated complexes were not stable and probabilities of its

formations were decreased by increasing temperatures [33].

Conclusion

The electro polymerization of the PAA and PAA Nano composites coating on MS was conducted by utilizing DC power supply method in aqueous solution (3.5% NaCl). The corrosion protection property of the polymer Nano composites coating in 3.5% NaCl solution was tested by potentiodynamic polarization. The corrosion current density (icorr) and corrosion potential (Ecorr) increased with increasing temperatures. The corrosion current density (icorr) lowered after coating on the MS with the polymer films in the presence and absence of the Nano materials. Tafel plot showed that corrosion potential (Ecorr) of the MS coated with the polymer film in the presence and absence of the Nano materials shift to noble direction in comparison with that of the uncoated MS, implying that the polymer film act as anodic protection. The polymer Nano composites coatings have excellent corrosion resistance because they achieve higher corrosion inhibition efficiency and protection efficiency (PE %) in comparison with bare MS, and that Nano composites materials could expand the applications in the field of anti-corrosion because of their simple preparation, stable performance, and good anti corrosion effects. SEM and AFM analyses revealed that the protection of MS took place because of the formations of protective films on the metal surface and exhibited better barrier effects.

Acknowledgements

References

[1] F. Alfinito, G. Ruggiero, M. Sica, A. Udhayachandran, V. Rubino, R. Della Pepa, A.T. Palatucci, M. Annunziatella, R. Notaro, A.M. Risitano, G. Terrazzano, *Immunobiology*, **2012**, *217*, 698–703. [crossref], [Google Scholar], [Publisher]

[2] S. De, J.L. Lutkenhaus, *Green Chem.*, **2018**, *20*, 506–514. [crossref], [Google Scholar], [Publisher]

[3] B. Fotovvati, N. Namdari, A. Dehghanghadikolaei, *J. Manuf. Mater. Process,* **2019**, *3*, 28. [crossref], [Google Scholar], [Publisher]

[4] A. Dehghanghadikolaei, B. Fotovvati, *Materials*, **2019**, *12*, 1795. [crossref], [Google Scholar], [Publisher]

[5] J.M. Pringle, O. Ngamna, J. Chen, G.G. Wallace, M. Forsyth, D.R. MacFarlane, *Synth. Met.,* **2006**, *156*, 979-983. [crossref], [Google Scholar], [Publisher]

[6] O.S. Yakovenko, L.Y. Matzui, L.L. Vovchenko, A.V. Trukhanov, I.S. Kazakevich, S.V. Trukhanov, Y.I. Prylutskyy, U. Ritter, *J. Mater. Sci.*, **2017**, *52*, 5345–5358. [crossref], [Google Scholar], [Publisher]

[7] A.H. Navarchian, M. Joulazadeh, F. Karimi, *Prog. Org. Coat.*, **2014**, *77*, 347–353. [crossref], [Google Scholar], [Publisher]

[8] A.M. Kumar, Z.M. Gasem, *Prog. Org. Coat.*, **2015**, *78*, 387–394. [crossref], [Google Scholar], [Publisher]

[9] B. Ramezanzadeh, G. Bahlakeh, M. Ramezanzadeh, *Corros. Sci.*, **2018**, *137*, 111–126. [crossref], [Google Scholar], [Publisher]

[10] G. Contri, G.M.O. Barra, S.D.A.S. Ramoa, C. Merlini, L.G. Ecco, F.S. Souza, A. Spinelli, *Prog. Org. Coat.*, **2018**, *114*, 201–207. [crossref], [Google Scholar], [Publisher]

[11] G. Zamiri, A.S.M.A. Haseeb, *Materials*, **2020**, *13*, 3311. [crossref], [Google Scholar], [Publisher]

[12] S.T. Skowron, I.V. Lebedeva, A.M. Popov, E. Bichoutskaia, *Chem. Soc. Rev.*, **2015**, *44*, 3143–3176. [crossref], [Google Scholar], [Publisher]

[13] R.A. Faris, Z.F. Mahdi, M.D.A. Husein, Immobilised Gold Nanostructures on Printing Paper for Lable-Free Surface-enhanced Raman Spectroscopy, *IOP Conf. Ser.: Mater. Sci. Eng.*, IOP Publishing Ltd, **2020**, 871, 012019. [crossref], [Google Scholar], [Publisher]

[14] Y. Jafari, S. Ghoreishi, M. Shabani-Nooshabadi, *Synth. Met.*, **2016**, *217*, 220–230. [crossref], [Google Scholar], [Publisher]

[15] Y.J. Wan, L.C. Tang, L.X. Gong, D. Yan, Y.B. Li, L.B. Wu, J.X. Jiang, G.Q. Lai, *Carbon*, **2014**,

69, 467–480. [crossref], [Google Scholar], [Publisher]

[16] A.S. Khulood, S.K. Khalil, I.K. Muna, *Journal of Pharmacy and Biological Sciences*, **2018**, *13*, 30-36. [Google Scholar]

[17] E. Léonard-Stibbe, G. Lécayon, G. Deniau, P. Viel, M. Defranceschi, G. Legeay, J. Delhalle, *J. Polym. Sci.: Part A, Polym. Chem.*, **1994**, *32*, 1551-1555. [crossref], [Google Scholar], [Publisher]

[18] E. Younang, E. Léonard-Stibbe, P. Viel, M. Defranceschi, G. Lécayon, J. Delhalle, *Molec. Engin*, **1992**, *1*, 317-332. [crossref], [Google Scholar], [Publisher]

[19] R.M. Silverstein, F.X. Webster, D.J. Kiemle, *Spectrometric Identification of Organic Compounds*, **2005**, 7th ed., John Wiley & Sons, Westford, US. [Pdf], [Google Scholar], [Publisher]

[20] R. Shirner, R. Fuson, D. Cartin, T. Mrril **1980**, *The Systematic Identification of Organic Compound*, 8th ed., John Wiley & Sons, Ne. [Publisher]

[21] N. Koj, **1962**, Infrared absorption spectroscopy, 1st ed., Nankodo Cmpany Limited, Tokyo. [Publisher]

[22] J. Zheng, L. Liu, G. Ji, Q. Yang, L. Zheng, J. Zhang, *ACS Appl. Mater. Interfaces*, **2016**, *8*, 20074-20081. [crossref], [Google Scholar], [Publisher]

[23] M.I. Ali, K.A. Saleh, Electropolymerization of N-Salicyly tetrahydro phthalamic acid for anticorrosion and antibacterial action applications, *IOP Conf. Ser.: Mater. Sci. Eng.*, IOP Publishing, **2019**, 571, 012072. [crossref], [Google Scholar], [Publisher]

[24] V. Divij, R.K. Goyal, *Materials Science and Engineering*, **2014**, *64*, 1-10.

[25] V. Alzari, D. Nuvoli, R. Sanna, S. Scognamillo, M. Piccinini, J.M. Kenny, G. Malucelli, A. Mariani, *J. Mater. Chem.*, **2011**, *21*, 16544–16549. [crossref], [Google Scholar], [Publisher]

[26] E. Heitz, W. Schwenk, *British Corrosion J.*, **1976**, *11*, 74-77. [crossref], [Google Scholar], [Publisher]

[27] K.R. Tretherwey, J. Chamberlain, *Corrosion for Science and Engineering*, 2nd ed. Addision Wesley Longman Ltd, **1995**. [Google Scholar]

[28] J.M. Saleh, Y.K. Al-Haidari, *Bull. Chem. Soc. Jpn.*, **1989**, *62*, 1237. [crossref], [Google Scholar], [Publisher]

[29] D. Enders, J.P. Shilvock, *Chem. Soc. Rev.*, **2000**, *29*, 359-373. [crossref], [Google Scholar], [Publisher]

[30] M. Fontana, N. Greene, **1986**. Corrosion engineering: New York: McGraw- Hill.

[31] M. Husaini, B. Usman, M.B. Ibrahim, *bayero J. Pure Appl. Sci.*, **2018**, *11*, 88-92. [crossref], [Google Scholar], [Publisher]

[32] M. Gomma, M. Wahdan, *Mater. Chem. Phys.*, **1995**, *39*, 209-213. [crossref], [Google Scholar], [Publisher]

[33] F. Mikdad Ahmed, S.M. Hassan, M.I. Kamil, *Iraqi Journal of Physics*, **2020**, *18*, 50-61. [crossref], [Google Scholar], [Publisher]